SAND2017-11799C

Probability Distribution of von Mises Stress in the Presence of Pre-Load

Daniel J. Segalman
Department of Mechanical Engineering
Michigan State University
East Lansing, MI 48824
segalman@egr.MSU.edu

Garth M. Reese
Computational Solid Mechanics and Structural Dynamics
Sandia National Laboratories*
Albuquerque, NM 87185-0380
gmreese@sandia.gov

Richard V. Field, Jr.
Mission Analytics Solutions
Sandia National Laboratories
Albuquerque, NM 87185-1027
rvfield@sandia.gov

ABSTRACT

Random vibration under preload is important in multiple endeavors, including those involving launch and re-entry. In these days of increasing reliance on predictive simulation, it is important to address this problem in a probabilistic manner - this is the appropriate flavor of quantification of margin and uncertainty in the context of random vibration. One of the quantities of particular interest in design is the probability distribution of von Mises stress. There are some methods in the literature that begin to address this problem, but they generally are extremely restricted and astonishingly, the most common restriction of these techniques is that they assume zero mean loads. The work presented here employs modal tools to suggest an approach for estimating the probability distributions for von Mises stress of a linear structure for the case of multiple independent Gaussian random loadings combined with a nonzero pre-load.

Key words: random vibration, von Mises stress, Gaussian, pre-load, stress process

NOMENCLATURE

$F(t)$	Vector of random dynamic loads applied to structure
F_0	Vector of static loads applied to structure
d	The number of applied random dynamic forces
$\mathscr{R}^d$	The d-dimensional space of real numbers
S_{qq}	cross spectral density matrix of modal displacements
$q(t)$	Column vector of modal displacements
$\sigma(x,t)$	Instantaneous stress at location x and time t
$\sigma_0(x)$	Static stress at location x
$\Psi(x)$	Matrix each of whose columns is the vector of stress components associated with that mode at that location (modal stresses)
$\Psi_n(x)$	The n^{th} column of $\Psi(x)$
N_M	The number of vibration modes retained for analysis
$p(x,t)$	von Mises stress at location x and time t
A	6x6 matrix mapping used to map stress vectors to von Mises stress
$B(x)$	$\Psi^T(x)A\Psi(x)$

*Sandia National Laboratories is a multi-mission laboratory managed and operated by National Technology and Engineering Solutions of Sandia, LLC., a wholly owned subsidiary of Honeywell International, Inc., for the U.S. Department of Energy's National Nuclear Security Administration under contract DE-NA-0003525.

Γ_{qq}	The zero-time lag covariance matrix of modal displacement: $E\left[qq^T\right]$
$p^2_{\text{RMS}}(x)$	Time average of the square of von Mises stress
Q	Element of decomposition $\Gamma_{qq} = QXQ^T$
N_R	The rank of Γ_{qq}
$\hat{q}(t)$	$QX\beta(t)$
$\beta(t)$	$X^{-1}Q^T q(t)$
C	$XQ^T BQX$
$R(x)$	Defined in decomposition $C(x) = R(x)D^2(x)R^T(x)$
$D(x)$	Defined in decomposition $C(x) = R(x)D^2(x)R^T(x)$
N_P	The number of stress processes
$y(t,x)$	$R^T(x)\beta(t)$
Y_0^2	$p_0^2 - \gamma^T D^2 \gamma$
γ	$G(x)\sigma_0(x)$
G	$-D^{-2}R^T X^T Q^T \Psi^T A$
L	Length of beam in first and second example problems
ρ_B	Density of beam in first and second example problems
w	Half width of beam in first and second example problems
PDF	Probability Density Function
CDF	Cumulative Distribution Function

1 INTRODUCTION

Random vibration under preload is important in multiple endeavors, including those involving launch and re-entry. In these days of increasing reliance on predictive simulation, it is important to address this problem in a probabilistic manner - this is the appropriate flavor of quantification of margins and uncertainties in the context of random vibration. There are some methods in the literature that only begin to address this problem:

1. Miles' equation [1] addresses the accelerations seen by a single degree of freedom system supported by a randomly driven base. The attachment stresses are presumed to be proportional to the relative displacements. This is, of course, not suitable for real physical systems containing multiple degrees of freedom.
2. A method of Segalman et. al. [2] facilitates estimating the RMS value of von Mises stresses under pre-load for arbitrary weakly stationary random dynamic loads, so long as the cross-spectral density matrix for load is available. This says nothing about probability distribution of von Mises stress.
3. Another method of Segalman et. al. [3] does provide a method for calculating the probability distribution of von Mises stress so long as the applied random dynamic loads are stationary Gaussian and there is no pre-load.
4. Tibbits [4] extended the method of [3] to the case where there is pre-load, but where only one random dynamic stress load is applied. Though a major advance, this still does not admit re-entry type cases - where non-uniform random dynamic loads are distributed spatially about the structure.

None of these methods can be employed to address the severe conditions of random vibration applied to a structure also subject to preload - for which launch or re-entry would be paradigms - and generate probabilistic expressions for the von Mises stress likely to be encountered.

An effort to achieving such a method is described in this monograph. The development here is based on results reported in a technical document [5] prepared while the first author was a member of technical staff of Sandia National Laboratories.

2 KEY INGREDIENTS

The most important ingredient to this development is the partition of the applied loads into a system of random dynamic loads $F(t)$ and a set of static pre-loads F^0. One might assume that the static loads are self-equilibrating, but the following development does not require that condition. Also, critical to the following development is the assumption that the random dynamic load components $F(t)$ are stationary Gaussian processes with zero mean.

Let $F(t)$ be an $\mathscr{R}^d$-valued, weakly stationary Gaussian process of zero mean and having correlation matrix $r_{FF}(\tau) = E\left[F(t)F(t+\tau)^T\right]$, a dxd matrix. The matrix of two-sided spectral densities [6] is denoted by $S_{FF}(\omega)$ [6]

$$S_{FF}(\omega) = \frac{1}{2\pi}\int_{\mathscr{R}} r_{FF}(\tau)\, e^{-i\omega\tau}\, d\tau. \tag{1}$$

This matrix defines the characterization of the input needed for random vibration studies, assuming a linear structure.

From $S_{FF}(\omega)$ plus the structure's frequency response functions we can derive the cross spectral density matrix of modal displacement $S_{qq}(\omega)$. From $S_{qq}(\omega)$ we can evaluate the Γ_{qq}, the zero-time lag covariance matrix of modal displacement. (Γ_{qq} is defined mathematically below and a useful development can be found in Appendix A of [5]).

In the following section, we show how knowing Γ_{qq} and assuming that all loads are Gaussian processes, we may determine the statistics of von Mises stress of a linear structure, even in the presence of pre-load.

3 SEPARATION OF STRESS RESPONSE DUE TO STATIC AND RANDOM VIBRATION LOADS

At each location x in the structure, we can express the stress vector (discussed more below) in terms of modal amplitudes

$$\sigma(t,x) = \sigma_0(x) + \sum_n q_n(t)\,\Psi_n(x) = \sigma_0(x) + \Psi(x)\,q(t), \tag{2}$$

where q is a column vector of modal amplitudes with coordinates q_n and $\Psi(x)$ is a matrix each of whose columns is the vector of stress components associated with that mode at that location (modal stresses). Vector $\Psi_n(x)$ is the n^{th} column of $\Psi(x)$. We have truncated the sum at N_M modes.

The square of the von Mises stress is

$$p^2(t,x) = \Big(\Psi(x)q(t) + \sigma_0(x)\Big)^T A \Big(\Psi(x)q(t) + \sigma_0(x)\Big), \tag{3}$$

where

$$A = \begin{bmatrix} 1 & -1/2 & -1/2 & 0 & 0 & 0 \\ -1/2 & 1 & -1/2 & 0 & 0 & 0 \\ -1/2 & -1/2 & 1 & 0 & 0 & 0 \\ 0 & 0 & 0 & 3 & 0 & 0 \\ 0 & 0 & 0 & 0 & 3 & 0 \\ 0 & 0 & 0 & 0 & 0 & 3 \end{bmatrix} \tag{4}$$

We expand the argument in Equation (3):

$$p^2(t,x) = \Big(\Psi(x)\,q(t)\Big)^T A \Big(\Psi(x)\,q(t)\Big) + \sigma_0^T(x) A\,\sigma_0(x) + \Big(\Psi(x)\,q(t)\Big)^T A\,\sigma_0(x) + \sigma_0^T(x) A \Big(\Psi(t)\,q(t)\Big). \tag{5}$$

Let $p_R^2(t,x)$ denote the component of squared von Mises stress due solely to random vibration, that is, the first term on the RHS of Equation (5). Then

$$p_R^2(t,x) = \Big(\Psi(x)\,q(t)\Big)^T A \Big(\Psi(x)\,q(t)\Big) = q(t)^T B(x)\,q(t), \tag{6}$$

where

$$B(x) = \Psi^T(x) A \Psi(x). \tag{7}$$

It follows that

$$E[p_R^2(t,x)] = B(x)_{ij} E[q_i q_j] = B(x)_{ij} \left(\Gamma_{qq}\right)_{ij} = \left(B(x)^T \Gamma_{qq}\right)_{jj} = \mathrm{Tr}\left(B^T(x)\,\Gamma_{qq}\right) \tag{8}$$

where

$$\Gamma_{qq} = E[q(t)\, q^T(t)] \tag{9}$$

is the zero-time lag covariance matrix of modal amplitude. (Summation on repeated indices was employed in Equation (8).) We note that Γ_{qq} has neither spatial or temporal dependence and that B has spatial dependence only. Also both matrices are symmetric, so the use of $()^T$ in Equation (8) is optional.

3.1 An intermediate result: RMS von Mises

Let's take the expected value of the right side of Equation (5) to find

$$p_{\mathrm{RMS}}^2(x) = E\left[p^2(t,x)\right] = E\left[q^T(t) B(x) q(t)\right] + 2E\left[q^T(t)\right] \Psi^T(x) A \sigma_0(x) + \sigma_0^T(x) A\, \sigma_0(x), \tag{10}$$

but $E[q] = 0$, so the difference between the square of RMS von Mises stress in the absence of pre-stress (Equation (8)) and the square of von Mises stress in the presence of pre-stress (Equation (10)) is the square of von Mises stress of the pre-load alone ($\sigma_0^T A \sigma_0$). Examining the un-squared von Mises stress, we see that

$$p_{\mathrm{RMS}}(x) = \sqrt{\mathrm{Tr}\left(B^T(x)\,\Gamma_{qq}\right) + \sigma_0^T(x) A\, \sigma_0(x)} \le \sqrt{\mathrm{Tr}\left(B^T(x)\,\Gamma_{qq}\right)} + \sqrt{\sigma_0^T(x) A\, \sigma_0(x)} \tag{11}$$

by the triangle inequality. Hence, the RMS von Mises stress is less than or equal to the sum of that due to random vibration and that due to preload.

3.2 Reduction to Stress Processes

Noting that matrix Γ_{qq} is square (N_MxN_M) and positive semi-definite, we may decompose it

$$\Gamma_{qq} = Q X^2 Q^T, \tag{12}$$

where X is a diagonal matrix whose dimension (N_R) is the rank of Γ_{qq} and Q is a rectangular matrix having the property that

$$Q^T Q = I_{N_R} \tag{13}$$

where I_{N_R} is the identity matrix of rank N_R. Note that because Γ_{qq} has no time or spatial dependence, neither do Q or X.

This permits us a change of variables

$$\beta(t) = X^{-1} Q^T q(t) \tag{14}$$

where, by construction,

$$E[\beta(t)\, \beta(t)^T] = I_{N_R} \tag{15}$$

so that the elements of β are independent, identically distributed random processes. (Proof of this requires that we recall that X is a diagonal matrix and $\beta(t)$ is a linear mapping of $F(t)$ and therefore Gaussian.) While Q is not generally invertible, we may introduce the new random vector

$$\hat{q}(t) = Q X \beta(t). \tag{16}$$

It is shown in Appendix B of [5] that q and $\hat{q}$ have identical first and second moments, and are therefore equivalent Gaussian random vectors. For the purpose of characterizing the statistics of von Mises stress, we could employ $\hat{q}$ in Equation (5) with the same legitimacy as employing q.

In our new coordinates β, the square of the von Mises stress *due solely to random vibration* is

$$p_R^2(t,x) = \beta^T(t)\, C(x)\, \beta(t), \tag{17}$$

where

$$C(x) = X^T\, Q^T\, B(x)\, Q X. \tag{18}$$

Matrix $C(x)$ is square, having dimensionality equal to the rank of Γ_{qq} but possibly much lower rank. The rank of C is the minimum of the rank of the matrices in the product on the right hand side of Equation (18). Note that rank(X) = dimension(X) = rank$(\Gamma_{qq}) = N_R$ and rank$(B) \leq$ rank$(A) = 5$.

We exploit the symmetry and the positive semi-definiteness of $C(x)$ in doing its singular value decomposition:

$$C(x) = R(x)\, D^2(x)\, R^T(x), \tag{19}$$

where the matrix $D(x)$ is diagonal and has dimension equal to the rank of N_P of $C(x)$, $R(x)$ is a rectangular matrix having property that $R^T R = I_{C(x)}$, and $I_{C(x)}$ is the identity matrix whose dimension is the rank of $C(x)$. We refer to N_P as the number of stress processes.

The square of the von Mises stress due solely to random vibration is now

$$p_R^2(t,x) = \beta^T(t)\, R(x)\, D^2(x)\, R^T(x)\, \beta(t). \tag{20}$$

This suggests yet another change of variables:

$$y(t,x) = R^T(x)\, \beta(t). \tag{21}$$

It is easily shown that the elements of y are independent, identically distributed (IID) Gaussian processes with unit variance. (This again employs the fact that X is a diagonal matrix and y is a linear function of F.) There are two obvious advantages of the above transformation: (1) it reduces the number of random variables of this problem to the rank of A (at most 5), and (2) it aligns the random variables in the directions of the axes of the ellipsoids of constant von Mises stress.

When Equation (21) is substituted into Equation (20), we obtain

$$p_R^2(t,x) = y(t,x)^T\, D(x)^2\, y(t,x) = \sum_n y_n(t,x)^2\, D_n(x)^2. \tag{22}$$

The above expression suggests the following terminology. We refer to the dimension of $D(x)$ as the number of independent 'stress processes' acting at the location x.

It is worthwhile to discuss how many modes should be retained in the above calculations. As in other cases of modal synthesis, one must include those modes whose frequency response functions significantly intersect the excitation spectrum. A conservative approach is to employ all modes through an upper bound of the frequencies in the power spectrum of the input loads. Since the largest computational effort involves the decomposition in Equation (12), and that need be done only once per load case, the cost of such conservatism is not unreasonable.

Let us now return to calculation of the full von Mises stress, as presented in Equation (5), but with our newer degrees of freedom, that is,

$$p^2(t,x) = y(t,x)^T\, D^2(x)\, y(t,x) + 2\, \beta(t)^T \left(X^T\, Q^T\, \Psi(x)^T \right) A\, \sigma_0(x) + \sigma_0(x)^T\, A\, \sigma_0(x). \tag{23}$$

Approximating[1]

$$\beta(t) \approx R(x) y(t,x) \tag{24}$$

[1] By this approximation, we mean that $y(t,x)^T \left(R(x)^T\, X\, Q^T\, \Psi(x)^T \right) A$ and $\beta(t)^T \left(X\, Q^T\, \Psi(x)^T \right) A$ have identical second moment properties.

TABLE 1: Global Matrices

	Γ_{qq}	X	Q	A
Dimension	$N_M \times N_M$	$N_R \times N_R$	$N_M \times N_R$	6×6
Character		Diag.		Rank 5

TABLE 2: Local Matrices

	Ψ	B	C	D	R	G	γ
Dimension	$6 \times N_M$	$N_M \times N_M$	$N_R \times N_R$	$N_P \times N_P$	$N_R \times N_P$	$N_P \times 6$	$N_P \times 1$
Character				Diag.			

at this location, we have

$$p^2(t,x) = y^T(t)\, D(x)^2\, y(t) + 2\, y(t)^T \left(R(x)^T\, X\, Q^T\, \Psi(x)^T \right) A\, \sigma_0(x) + \sigma_0(x)^T\, A\, \sigma_0(x). \tag{25}$$

Defining a vector $\gamma(x)$ by

$$\gamma(x) = G(x)\, \sigma_0(x), \tag{26}$$

where

$$G(x) = -D(x)^{-2} R(x)^T\, X\, Q^T\, \Psi(x)^T\, A \tag{27}$$

and $p_0^2(x) = \sigma_0^T(x) A \sigma_0(x)$, Equation (25) becomes

$$p^2(t,x) = y^T(t)\, D(x)^2\, y(t) - 2\, y(t)^T\, D(x)^2\, \gamma(x) + p_0(x)^2. \tag{28}$$

Obviously, this calls for completing the square

$$p^2(t,x) = (y(t) - \gamma(x))^T\, D(x)^2\, (y(t) - \gamma(x)) + Y_0(x)^2 \tag{29}$$

where

$$Y_0(x)^2 = p_0(x)^2 - \gamma(x)^T\, D(x)^2\, \gamma(x). \tag{30}$$

It appears that if $\sigma_0(x)$ is in the span of the vectors of $\Psi(x)$, $Y_0(x) = 0$. Otherwise $Y_0(x) > 0$.

The dimensions of the above matrices are presented in Tables 1 and 2. The dimensions themselves are discussed in Table 3.

TABLE 3: Dimensions

N_M	Number of modes employed
N_R	Rank of Γ_{qq}. $N_R \leq N_M$
N_P	Rank of C = number of random stress processes. $N_P \leq \text{rank}(A) = 5$

4 PROBABILISTIC STATEMENTS ON VON MISES STRESS

The statistics of the von Mises stress are determined via appropriate integration over the joint probability distribution of the coordinates of $y(t,x)$ defined by Equation (21).

4.1 A Previous Result from New Perspective

For instance we re-examine the mean square of the von Mises stress

$$E[p^2(t,x)] = \int_{-\infty}^{\infty} \cdots \int_{-\infty}^{\infty} p^2(t,x) \prod_r \rho_r(y_r)\, \mathrm{d}y_r = \int_{-\infty}^{\infty} \cdots \int_{-\infty}^{\infty} \left((y-\gamma(x))^T D(x)^2 (y-\gamma(x)) + Y_0(x)^2 \right) \prod_r \rho_r(y_r)\, \mathrm{d}y_r$$
$$= \mathrm{Tr}(D(x)^2) + p_0(x)^2, \tag{31}$$

where

$$\rho_r(y_r) = \frac{1}{\sqrt{2\pi}} e^{-y_r^2/2} \tag{32}$$

is the probability density function of a standard Gaussian random variable. For more detail on this derivation, please refer to Appendix C of [5]. We see that $D_r(x)^2$ is the contribution of the r^{th} random process to $E[p(t,x)^2]$ at location x and the rank of D is N_P, the number of independent random processes contributing to the von Mises stress response at that location.

4.2 Probability Distributions of von Mises Stress

To determine the probability law for $p(x,t)$, it is useful to work with the square of the von Mises stress. Further, because von Mises stress is non-negative, it follows that for any Y, we have $P(p \le Y) = P(p^2 \le Y^2)$. The probability that the square of von Mises stress amplitude is less than or equal to a quantity Y^2 is

$$F_Y = P(p^2 \le Y^2) = \begin{cases} 0 & \text{for} \quad Y \le Y_0 \\ \int_{Z(\{D\},\gamma,Y_0,Y)} \prod \rho_r(y_r) dy_r & \text{for} \quad Y > Y_0 \end{cases} \tag{33}$$

where $Z(\{D\},\gamma,Y_0,Y)$ is the N_P-dimensional ellipsoid containing points y associated with the square of the von Mises stress less than or equal to Y^2, that is

$$Z(\{D\},\gamma,Y_0,Y) = \left\{ y : ((y-\gamma)^T D^2 (y-\gamma)) \le Y^2 - Y_0^2 \right\} \tag{34}$$

and N_P is the rank of matrix D. Note that all the arguments of Z are functions of x only and that $Z(\{D\},\gamma,Y_0,Y)$ is an ellipsoid centered at γ. The semi-axes of these ellipsoids are

$$A_r = \sqrt{\frac{Y^2 - Y_0^2}{D_r^2}} \tag{35}$$

See Figure 1. (It is because von Mises stress is positive that the condition $p \le Y$ is equivalent to $p^2 \le Y^2$ and we are able to define Z without explicit use of square roots.)

The integral of Equation (33) is generally impossible to evaluate exactly, but approximate quadrature is straightforward. Here we employ a numerical quadrature similar to the heuristic used in explaining Riemann integration.

4.3 Quadrature by Boxes

One of the few domain types over which we can integrate Gaussian distributions is boxes in N space. Let B_λ be one such box, then

$$\int_{B_\lambda} \prod_{r=1}^{N_P} \rho_r(y_r)\, dy_r = \prod_{r=1}^{N_P} \left[\Phi(y_{r,\max}) - \Phi(y_{r,\min}) \right], \tag{36}$$

where $y_{r,\max}$ and $y_{r,\min}$ define the boundaries of B_λ, and

$$\Phi(x) = \frac{1}{\sqrt{2\pi}} \int_{-\infty}^{x} \exp(-s^2/2)\, \mathrm{d}s. \tag{37}$$

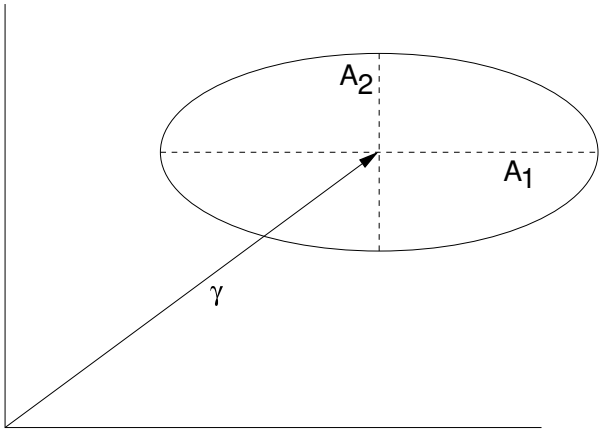

Figure 1: *Regions of constant von Mises stress are ellipsoids centered at locations γ.*

Note that Φ can also be expressed in terms of the error function, that is, $\Phi(x) = (1/2)\left(1 + \mathrm{erf}(x/\sqrt{2})\right)$.

Because $Z(\{D\}, \gamma, Y_0, Y)$ is a convex volume, it is easy to devise sequences of sets of boxes that are fully contained in $Z(\{D\}, \gamma, Y_0, Y)$ but whose net volume converge to that of $Z(\{D\}, \gamma, Y_0, Y)$ from below. Similarly, it is straightforward to define sequences of sets all of which contain $Z(\{D\}, \gamma, Y_0, Y)$, and whose volumes converge to that of $Z(\{D\}, \gamma, Y_0, Y)$ from above (see Figure 2).

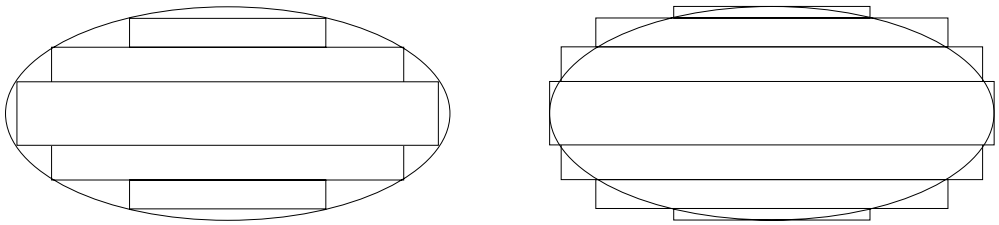

Figure 2: *Sets of boxes comprising subsets and supersets of the volume $Z(\{D\}, \gamma, Y_0, Y)$ for the case of $N_P = 2$.*

For the following examples, the above integration over N-dimensional ellipsoids was performed via recursive calls to Matlab® function codes to obtain both upper and lower bounds for the integral defined by Equation (33). (Listings can be found in Appendix D of [5].)

Credit should be given to Tibbits [4], [7] for creating approaches to the calculation of probability distribution for von Mises stress in the presence of pre-stress, but with some limitations. The approaches developed by Tibbits do not appear to accommodate the possibility of the number of random stress processes being less than the rank of the stress vector. The applications were limited to two dimensional problems where that assumption might more often be valid.

4.4 An Upper Bound for von Mises Probability

The recursive integrations associated with calculation of the probability distribution of von Mises stress where there are more than one random stress process present might be off-putting. Here we consider an obvious upper bound.

Let $B_U(\{D\},\gamma,Y_0,Y)$ be the smallest N-box that entirely contains $Z(\{D\},\gamma,Y_0,Y)$, that is

$$Z(\{D\},\gamma,Y_0,Y) \subset B_U(\{D\},\gamma,Y_0,Y). \tag{38}$$

The length of each side of the B_U will be twice a semi-axis of Z. Because of Equation (38)

$$\int_{Z(\{D\},\gamma,Y_0,Y)} \prod \rho_r(y_r)\,\mathrm{d}y_r \leq \int_{B_U(\{D\},\gamma,Y_0,Y)} \prod \rho_r(y_r)\,\mathrm{d}y_r = \prod_{r=1}^{N_P} \left[\Phi(y_{r,\max}) - \Phi(y_{r,\min})\right], \tag{39}$$

where in this case $y_{r,\max}$ and $y_{r,\min}$ identify the coordinates at the corners of B_U.

4.5 Strategy for Implementation in a Finite Element Setting

Referring to Equations (33) and (34) and then backwards to Equations (26) and (30), we see that the necessary ingredients for computing the probability distribution at any location are $D(x)$, $G(x)$, and $\sigma_0(x)$.

The simplest strategy would be to implement the calculations, so much as possible, via post processing. The element variables D and G would come most naturally from a linear structural dynamics code, such as Salinas [8] or NASTRAN [9]. Because D is diagonal and has at most 5 rows, the storage of it at each quadrature point is not an issue. Matrix G has at most 5 rows and 6 columns, and storage space at each quadrature point should be quite manageable. Salinas is mentioned specifically because it lends itself to modification by the authors and MSC NASTRAN is mentioned because of its DMAP capability [10]. The static stresses, σ_0 - and there might be ensembles of them - can come from a linear or nonlinear quasi-static analysis code.

There are a few more considerations:

- One caveat in employing results from different finite element codes is the requirement that the meshes and coordinate systems must be identical. Additionally, conventions on stress orientation must be the same.
- The ordering of rows of D and G should be that of the development above: diagonal terms of D in decreasing order and each row of G as defined in Equation (27).
- Because it is likely that D will be stored as a 5x1 vector and G will be stored as a 5x6 matrix, regardless of how many stress processes actually exist at the corresponding quadrature point, it would be helpful to store $N_P(x)$, the number of stress processes as well.

5 EXAMPLE PROBLEMS

5.1 Example Problem 1

Consider the simply supported beam shown in Figure 3, consisting of a beam subject to a static compressive load F_0 applied longitudinally and two dynamic loads $F_1(t)$ and $F_2(t)$ applied laterally. Loads F_1 and F_2 are assumed independent, stationary Gaussian processes with zero mean. The beam will be of length L, width $2w$, density ρ_B, cross-sectional area A_B, and Young's modulus E.

In general, each of F_1 and F_2 would excite many modes, but for the purpose of illustration, we assume that the frequency content of F_1 is band limited so as to excite only the first bending mode of the beam and that the frequency content of F_2 is also band limited, but so as to excite only the second bending mode.

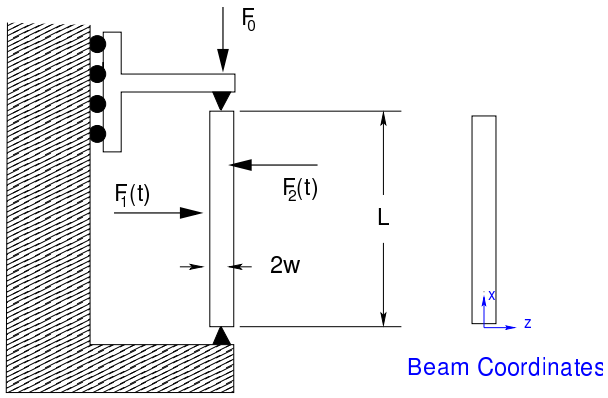

Figure 3: *Test case consisting of a simply supported beam of square cross section subject to a compressive longitudinal load F_0 and two random dynamic loads, $F_1(t)$ and $F_2(t)$ applied laterally.*

The static stress at any place on the beam is

$$\sigma_0 = \left\{ \begin{array}{c} -F_0/A_B \\ 0 \\ 0 \\ 0 \\ 0 \\ 0 \end{array} \right\} \tag{40}$$

with $F_0/A_B = 1$. For convenience with respect to expressing the stresses associated with the bending modes, we assume that all constants are scaled such that

$$Ew \left(\frac{\pi}{L}\right)^2 \sqrt{\left(\frac{2}{\rho_B A_B L}\right)} = 1. \tag{41}$$

The stress due to bending of any mode $n \in (1,2)$ is

$$\Psi(x,z) = \left\{ \begin{array}{cc} \sin\left(\frac{\pi x}{L}\right)\left(\frac{z}{w}\right) & 4\sin\left(\frac{\pi 2x}{L}\right)\left(\frac{z}{w}\right) \\ 0 & 0 \\ 0 & 0 \\ 0 & 0 \\ 0 & 0 \\ 0 & 0 \end{array} \right\} \tag{42}$$

where coordinates x and z are as indicated in Figure 3. Note that because the random loads generate only one component of stress (σ_1) we anticipate at most one random process to show up in the calculation of von Mises stress. Again, for purpose of illustration for this problem, we assume

$$\Gamma_{qq} = \left[\begin{array}{cc} 1 & 0 \\ 0 & 1/4 \end{array} \right] \tag{43}$$

The spatial distribution of RMS von Mises stress, that is, $p_{\text{RMS}}(x,z)$ defined by Equation (11), is illustrated on the upper section of Figure 4. Also shown on the lower section of the figure is $N_P(x,z)$, the rank of matrix $C(x,z)$ defined by Equation (18), which describes the number of stress processes acting at that location. Because all of the modes associated with the random loads have nodal lines at the top and bottom of the beam, there are no random processes at those locations.

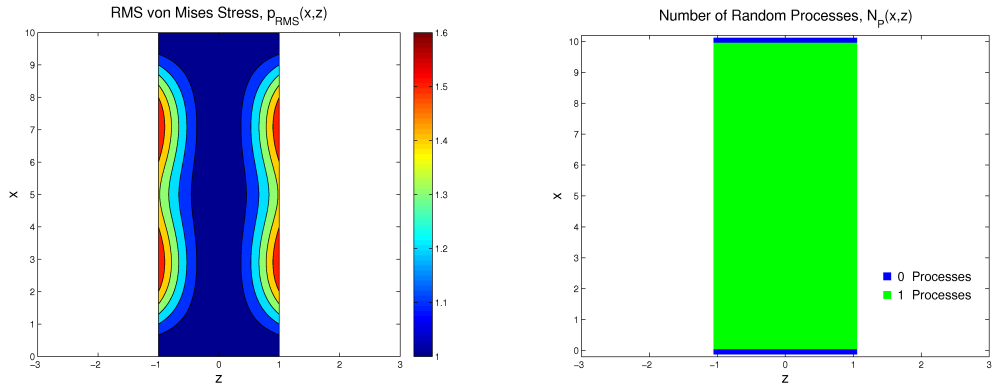

Figure 4: *The computed RMS von Mises stress resulting from the static pre-load and the lateral random dynamic loads is shown on the left. The distribution of the number of random processes is shown on the right.*

The RMS von Mises stress might be considered a nominal stress level, but one is perhaps more concerned about the probability of von Mises stress reaching high levels. The cumulative distribution function for von Mises stress is given by Equation (33). Suppose we are interested the 90th and 95th percentile of von Mises stress, that is, the values for Y such that the CDF defined by Equation (33) equals 0.9 and 0.95, respectively. Let Y_{90} and Y_{95} denote these values. The distributions of 90^{th} percentile and 95^{th} percentile von Mises stress are shown in Figure 5. The range of von Mises stress in Figure 5 is about twice that of the plot of RMS von Mises stress.

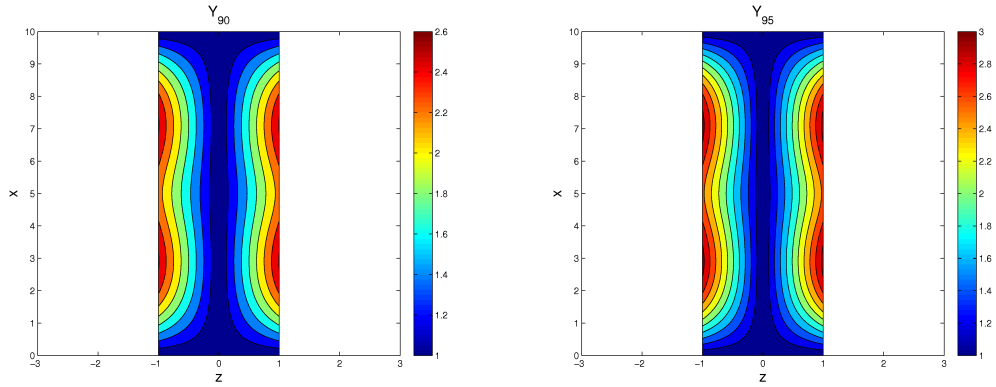

Figure 5: *The distribution of 90^{th} percentile and 95^{th} percentile von Mises stress are shown on the left and right contour plots, respectively.*

5.2 Example Problem 2

Consider the cantilevered/simply supported beam shown in Figure 6, subject to a static compressive load F_0 applied longitudinally, random dynamic load $F_1(t)$ also applied longitudinally, and random dynamic load $F_2(t)$ applied laterally at the free end of the beam. Loads F_1 and F_2 are assumed independent, stationary Gaussian processes with zero mean. The beam will be of length L, width $2w$, density ρ_B, cross-sectional area A_B, and Young's modulus E.

We consider two axial modes excited by load F_1 and one bending load excited by F_2. Each of F_1 and F_2 excite many modes, but for the purpose of illustration, we associate the first two axial modes with F_1 and the first bending mode with F_2, and ignore the rest. Here we assume that the beam is sufficiently short so that shear stresses associated with that bending mode are significant.

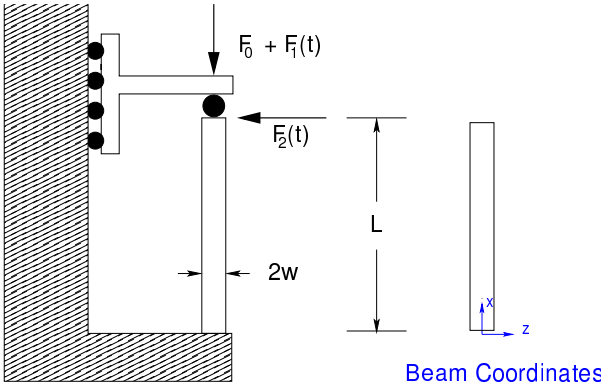

Figure 6: *Test case consisting of a cantilevered beam subject to a static compressive load F_0 applied longitudinally, random dynamic load $F_1(t)$ also applied longitudinally, and random dynamic load $F_2(t)$ applied laterally at the free end of the beam.*

Again, for convenience, we scale all constants such that Equation (41) holds, but this time to simplify the expression for stress associated with axial deformation. The first bending mode can be approximated by

$$u(x) = \frac{1}{24}\left(\frac{x}{L}\right)^2\left[\left(\frac{x}{L}\right)^2 - 4\left(\frac{x}{L}\right) + 6\right] \tag{44}$$

and we assume that the geometric features permit the scaling of bending stress shown below. The matrix of modal stresses $\Psi(x,z)$ is a 6x3 array with only 4 non-zero elements:

$$\begin{aligned}
\Psi_{11}(x,z) &= \frac{1}{2}\cos\left(\frac{\pi x}{2L}\right), \quad \Psi_{12}(x,z) = \frac{3}{2}\cos\left(\frac{\pi 3x}{2L}\right) \\
\Psi_{13}(x,z) &= \frac{1}{2}\left[1-\left(\frac{x}{L}\right)^2\right] - \left(\frac{x}{L}\right)\left[1-\left(\frac{x}{L}\right)\right]\frac{z}{w} \\
\Psi_{43}(x,z) &= \delta\left[1-\left(\frac{x}{L}\right)\right]\left(1-\left(\frac{z}{w}\right)^2\right)
\end{aligned} \tag{45}$$

where $\delta = I_B/(2Lw_BA_B)$, which for this example we set to $1/2$.

The static stress at any place on the beam is again

$$\sigma_0 = \left\{\begin{array}{c} -F_0/A_B \\ 0 \\ 0 \\ 0 \\ 0 \\ 0 \end{array}\right\} \tag{46}$$

where $F_0/A_B = 1$. Again, for purpose of illustration for this problem, we assume a simple form for Γ_{qq}:

$$\Gamma_{qq} = \left[\begin{array}{ccc} 1 & 0 & 0 \\ 0 & 1 & 0 \\ 0 & 0 & 3 \end{array}\right] \tag{47}$$

The RMS von Mises stress distribution for this case is shown on the upper part of Figure 7 and the distribution of the number of random processes is shown on the lower portion of that figure. Because all of the vibration modes

associated with the random loads have nodal lines at the top of the beam, there are no random processes there. On the left and right sides of the beam, there are only axial stress components, so there can be at most one process. In the interior of the beam, there are axial stress components due to the axial modes and the bending mode and there is a shear component associated with the bending, making two random stress processes possible.

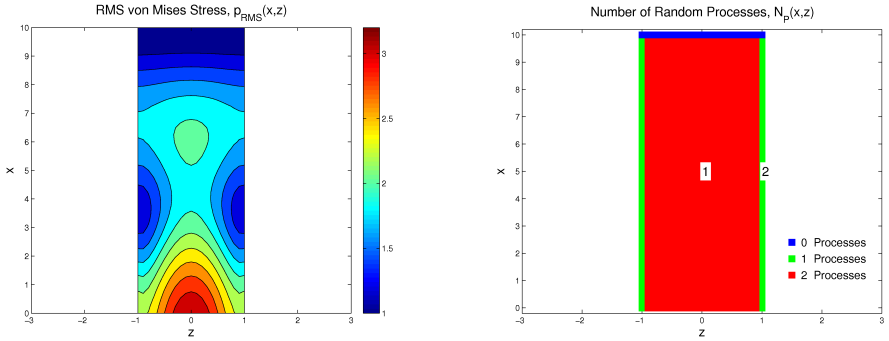

Figure 7: *The computed RMS von Mises stress resulting from the static pre-load and the lateral random dynamic loads is shown on upper graphic. The distribution of the number of random processes is shown below. The locations marked "1" and "2" are discussed above.*

Again, we are interested in the RMS von Mises stress, but also concerned about the probability of von Mises stress reaching high levels. The cumulative distribution function (CDF) for von Mises stress defined by Equation (33) are illustrated by Figure 8 for locations 1 and 2. For the case of a single random stress process (such as location 2), the upper bound as described by Equation (39) is exact. More of the character of these distributions are indicated by the Probability Density Functions (PDF) shown in Figure 9 for locations 1 and 2 noted in Figure 7. The PDF for location 1 has a shape typical where there are two random stress processes and the PDF for location 2 has a shape typical where there is only one random stress process [3].

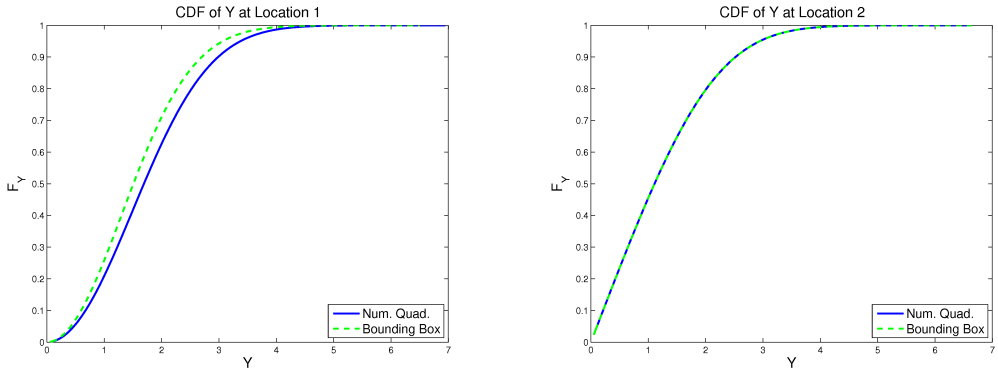

Figure 8: *The cumulative distribution functions (CDF) of von Mises stress at locations 1 and 2 are shown on the left and right graphics, respectively. Also shown are upper bounds obtained via Equation* (39)*. For the case of a single random stress process (such as location 2), the upper bound is exact.*

The spatial distributions of 5^{th} percentile, 50^{th} percentile, and 95^{th} percentile von Mises stress are shown in Figure 10. As expected, the range of von Mises stress in the 95^{th} percentile plot (right side of Figure 10) is substantially larger than those of the plot of RMS von Mises stress. The 5^{th} percentile plot is particularly interesting; because the random loads excite vibration that result in stresses that are co-linear with the static stresses, there will be occasion

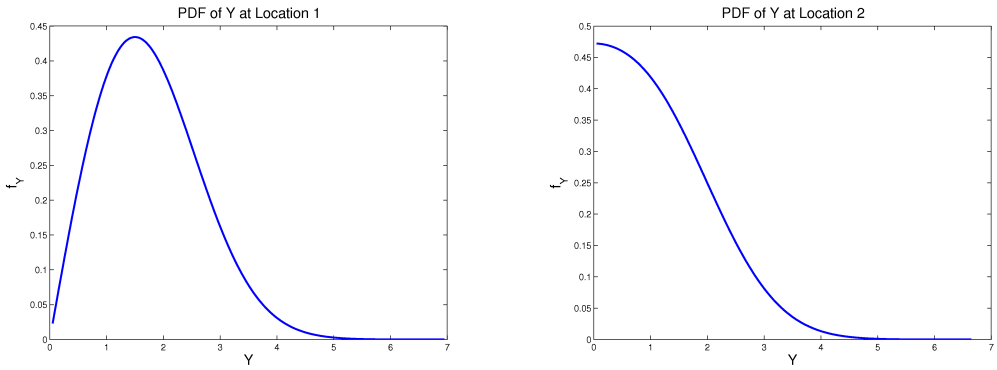

Figure 9: *The probability density functions (PDF) of von Mises stress at locations 1 and 2 are shown on the left and right, respectively.*

when the random stresses act in direction opposite to the static stresses resulting in von Mises stresses less than that associated with the static loads alone. The plot of 50^{th} percentile von Mises stress is very different from the RMS von Mises stress; this is the difference between the square root of the time average of a quadratic or a random variable, and the median of the absolute value of that variable.

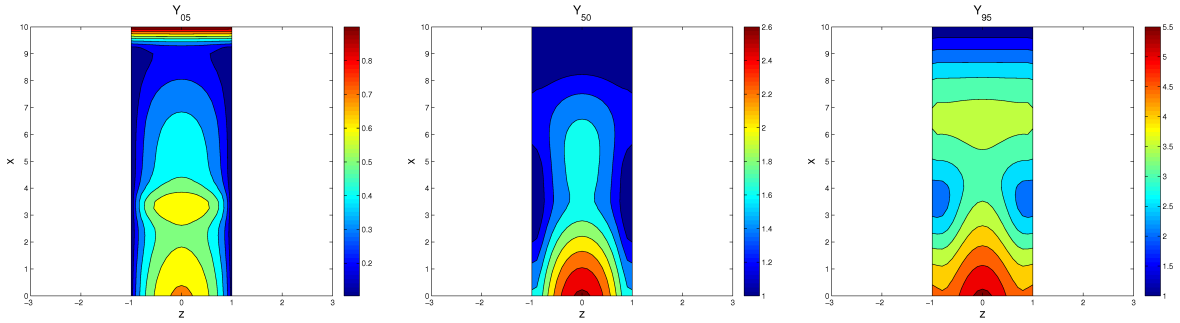

Figure 10: *The distribution of 5^{th} percentile, 50^{th} percentile, and 95^{th} percentile von Mises stress are shown on the left, middle, and right contour plots, respectively.*

6 SUMMARY

The necessity of considering the von Mises stress (effective stress) in cases of random vibration is long known. Incorporating predictive mechanics of random vibration into modern engineering decision making requires expressing the stress response in a probabilistic manner. Though some progress in this direction has been reported in the literature, there are serious gaps with respect to the technology necessary to address random vibrations under pre-load — such as the random vibration of decelerating space structures in atmospheric re-entry.

A significant improvement in capability is presented here. With the use of the standard elements of random vibration analysis (cross spectral density matrix of loads, the modal frequency response matrices, assumption of a stationary and Gaussian load, etc.), a formulation is presented to express the probability distribution of von Mises stress at any location on a linear structure even for cases where the structure is subject to an arbitrary distribution of *in situ* stress.

The formulation is not complicated and implementation in a finite element context appears to be straightforward.

On the other hand, evaluation of the necessary integrals can be compute intensive. A preferred implementation might involve the initial calculation of the full field of RMS von Mises stress and then calculation of the probability distribution of von Mises stress only at the “hot spots”.

Finally, it should be emphasized that the validity of the approximation embodied in Equation (24) is still an issue for investigation.

ACKNOWLEDGMENTS

The authors express our appreciation to David Day, of Sandia National Laboratories, for very helpful mathematical discussion about the approximation central to this work.

REFERENCES

[1] **Miles, J. W.**, *On Structural Fatigue Under Random Loading*, Journal of the Aeronautical Sciences, Vol. 21, No. 11, pp. 753–762, November 1954.

[2] **Segalman, D. J., Fulcher, C. W. G., Reese, G. M.** and **Field, R. V.**, *An efficient method for calculating R.M.S. von Mises stress in a random vibration environment*, Journal Of Sound And Vibration, Vol. 230, No. 2, pp. 393–410, Feb 17 2000.

[3] **Segalman, D. J., Reese, G., Field Jr, R.** and **Fulcher, C.**, *Estimating the probability distribution of von Mises stress for structures undergoing random excitation*, Journal of Vibration and Acoustics, Vol. 122, No. 1, pp. 42–48, 2000.

[4] **Tibbits, P. A.**, *Application of Algorithms for Percentiles of von Mises Stress From Combined Random Vibration and Static Loadings*, Journal of vibration and acoustics, Vol. 133, No. 4, 2011.

[5] **Segalman, D. J., Field, R. V.** and **Reese, G. M.**, *Probability distribution of von Mises stress in the presence of pre-load*, Tech. Rep. SAND2013-3429, Sandia National Laboratories, Albuquerque, NM, April 2013.

[6] **Roberts, J.** and **Spanos, P.**, Random vibration and statistical linearization, Dover Publications, 2003.

[7] **Tibbits, P. A.**, *Percentiles of von Mises Stress from Combined Random Vibration and Static Loading by Approximate Noncentral Chi Square Distribution*, ASME Journal of Vibration and Acoustics, Vol. 134, No. 4, pp. 41009, 2012.

[8] **Reese, G., Bhardwaj, M. K.** and **Walsh, T.**, *Salinas Theory Manual*, Sandia report SAND2004-4079, Sandia National Laboratories, PO Box 5800, Albuquerque, NM 87185, August 2004.

[9] **Lahey, R., Miller, M.** and **Reymond, M.**, MSC/NASTRAN Reference Manual, Version 68, The MacNeal-Schwendler Corporation, 1994.

[10] **Bella, D.** and **Reymond, M.**, MSC/NASTRAN DMAP Module Dictionary, MacNeal–Schwendler, Los Angeles, CA, 1997.